DYNAMIC BEHAVIOUR OF METAL VAPOUR IN ARC PLASMA DURING TIG WELDING

M. Tanaka, Y. Tsujimura and K. Yamazaki

ABSTRACT

In the present paper, the mechanism of metal vapour in arc plasma is discussed through the dynamic observation of spectra of helium, chromium, manganese and iron during stationary TIG welding of stainless steel. Wavelengths from 400 nm to 700 nm are observed by a monochromator with a diffraction grating. Radiation from the arc is sent to the monochromator through optical lens and spectroscopic images are captured with 500 fps by a high-speed digital video camera. Spectra of metal elements exist locally in the arc plasma due to the dependence on plasma temperature, and also the intensive region of each metal spectrum depends on the kinds of metal elements. Most part of metal vapour produced from the weld pool surface is carried on the cathode jet and then swept away towards surroundings of the arc. However, if the driving force like diffusion in plasma is large, some metal elements can get across the cathode jet and then can be carried on the circulation flow towards the tungsten electrode.

IIW-Thesaurus keywords: Electric arcs; GTA welding; Plasma; Spectroscopy; Vapours.

1 Introduction

Free-burning arcs are widely used in industrial applications, including arc welding [1], plasma spraying [2], plasma cutting [3] and so on. Many researchers have devoted experimental and theoretical efforts to understanding the physical characteristics of the arcs. These efforts helped to attain the practical understanding of the arc column and several books on arc physics have been published [4-6]. One of the practical understandings is the effects of metal vapour. For example, metal vapour emanating from the electrodes contributes to the self-stabilization of arcs and also to the reduction of the anode fall, with the result that the arc voltage decreases. The presence of metal vapour in the arc is inevitable in applications like arc welding because of the high temperature of the weld pool. The transport of metal vapour in the arc plasma is an important subject for investigation, since the vapour changes the arc properties, and therefore the properties of the weld pool. Many researchers have made a variety of investigations on metal-contaminated arc plasma [7-14]. Many studies on the effects of metal vapour have been reported and they make clear that the presence of metal vapour in the arc is an important factor of the arc properties. However, experimental observations of process and diffusion for a mixture of arc plasma and metal vapour from the weld pool have not been reported.

In the present paper, a spectroscopic analysis of helium and metal spectra is conducted in arc welding. The purpose of this paper is to clarify the mechanism of a mixture of metal vapour in the arc plasma.

2 Experimental method

The TIG (Tungsten Inert Gas) arc is struck in a pure helium atmosphere between a tungsten electrode and a flat stainless steel piece, SUS304, and then stationary TIG welding is carried out for 20 s after the arc ignition. The tungsten electrode, 3.2 mm in diameter, is ground to a conical tip angle of 60°. The TIG arc is operated at a current of 150 A, and the distance between electrodes is 3 mm.

Figure 1 shows a schematic drawing of the spectroscopic analysis system for this study. Wavelengths from 400 nm to 700 nm can be observed by a monochromator. The monochromator is the Czerny-Turner type and has diffraction grating with wavelength resolution 0.4 nm. Radiation from the arc is sent to the monochromator through the optical lens and spectroscopic images are captured with 500 fps by a high-speed digital videocamera (FACTCAM-512PCI, Photron). In this experiment, the spectra of HeI, CrI, MnI, FeI, CrII and FeII are observed. The MnII spectrum could not be observed because of the undetectable wavelength due to UV rays. The above wavelengths employed in this study are given in Table 1 [15, 16].

3 Observations at thermal plasma

Figures 2 to 5 show experimental results of spectroscopic images of HeI, CrI, MnI and FeI spectra. The intensity of the HeI spectrum weakens with passing time. Table 2 shows

Doc. IIW-2219, recommended for publication by Study Group SG-212 "The Physics of Welding."

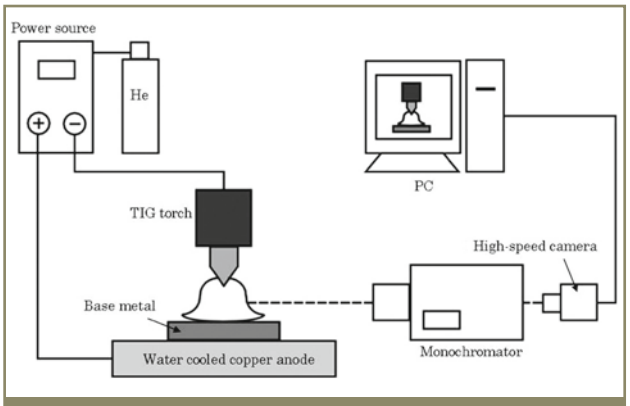

Figure 1 – Schematic drawing of the spectroscopic analysis system

excitation energies of each spectrum [18] and Figure 6 shows the dependence of normalized radiant intensities on temperature [18, 19]. The excitation energy of HeI is the very highest in Table 2 and the temperature region for HeI spectrum emission is much higher than other spectra. The plasma temperature decreases due to the effects of metal vapour which has generally low excitation energies. Therefore, helium is not able to be excited and the bright region of HeI shrinks and then disappears at 19 s after arc ignition.

CrI, MnI and FeI spectra do not exist in the arc plasma in the same manner. Intensities of CrI and MnI spectra are very strong in the arc column, but the FeI spectrum can be observed only close to the weld pool surface. It is suggested that existential location of metal vapour in the arc plasma depends on the kinds of metal elements. It is also expected that chromium and manganese exist inside the arc plasma, but iron is swept away toward the surroundings of the arc plasma.

Table 1 – Wavelengths of HeI, CrI, MnI, FeI, CrII and FeII spectral lines

Particle	Wavelength [nm]
Helium atom (HeI)	587.6
Chromium atom (CrI)	520.8
Manganese atom (MnI)	476.2
Iron atom (FeI)	538.3
Chromium ion (CrII)	455.9
Iron ion (FeII)	458.4

Table 2 – Excitation energies of HeI, CrI, MnI and FeI particles

Particle	Excitation energy [eV]
HeI 587.6 nm	23.07
CrI 520.8 nm	3.32
MnI 476.2 nm	5.49
FeI 538.3 nm	6.61

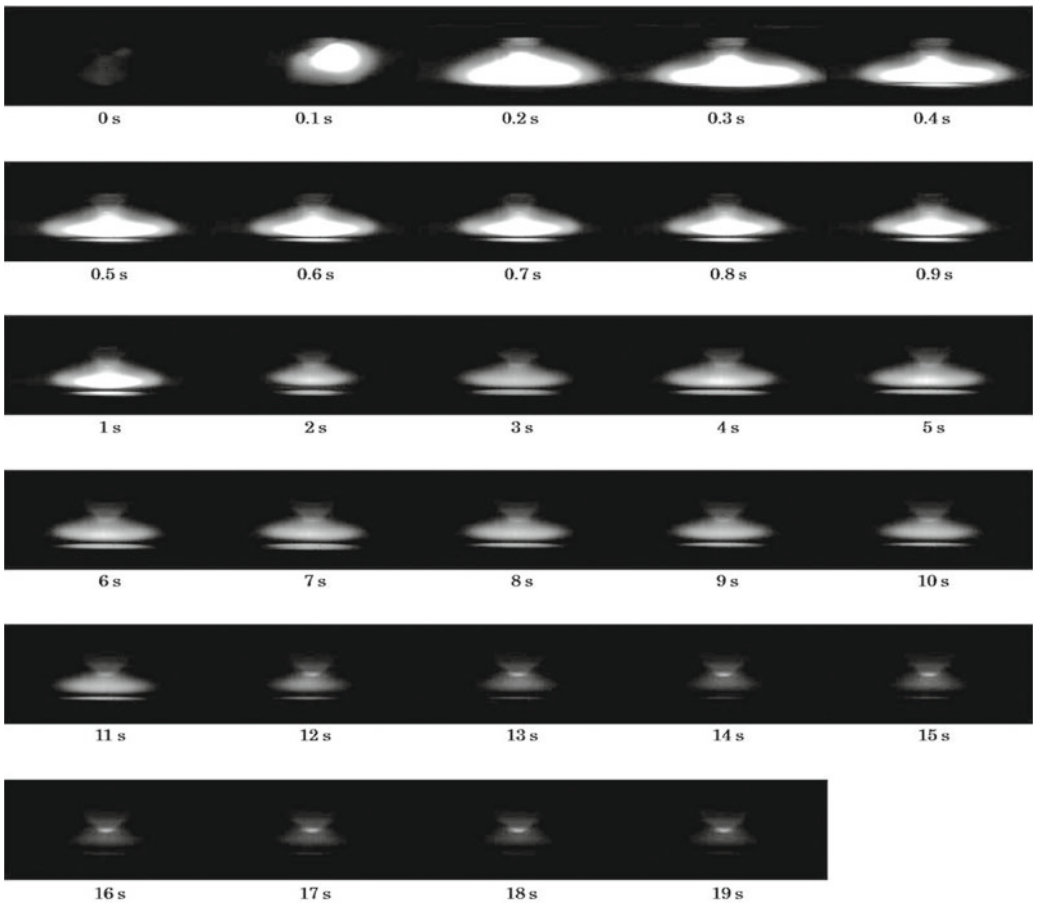

Figure 2 – Photographs of HeI spectrum in arc during helium TIG welding of stainless steel

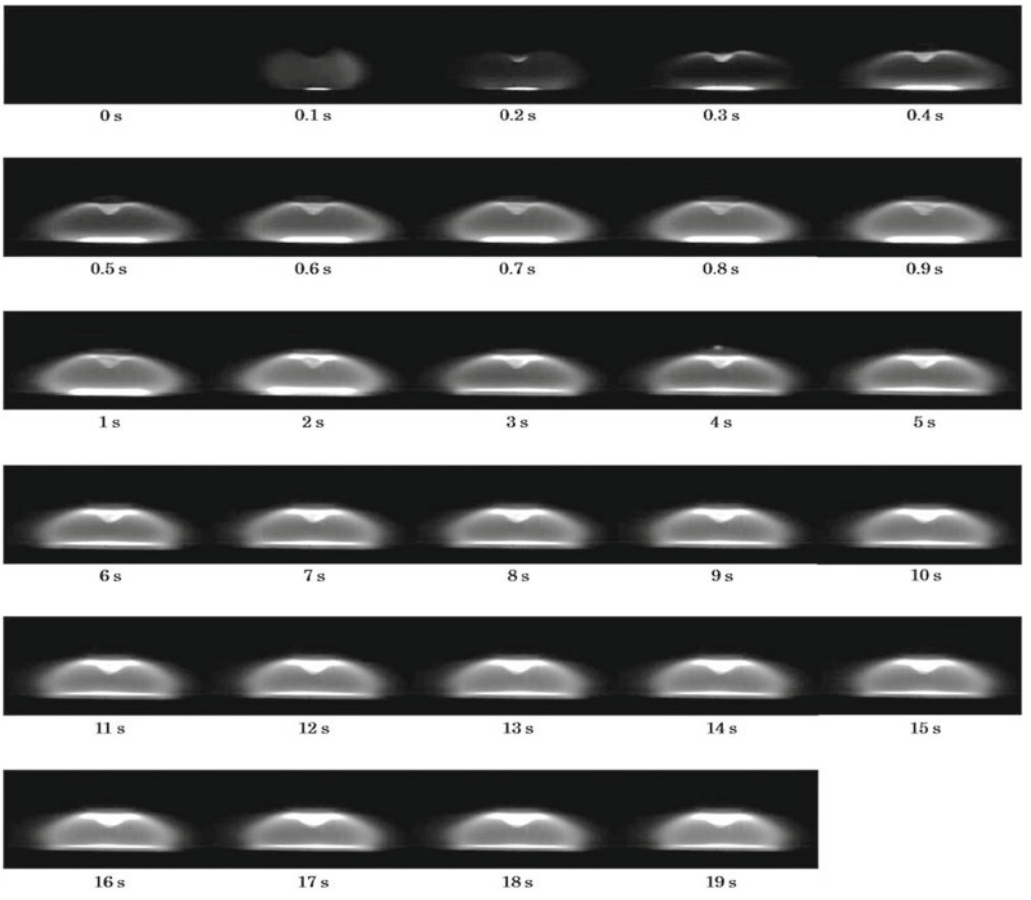

Figure 3 – Photographs of CrI spectrum in arc during helium TIG welding of stainless steel

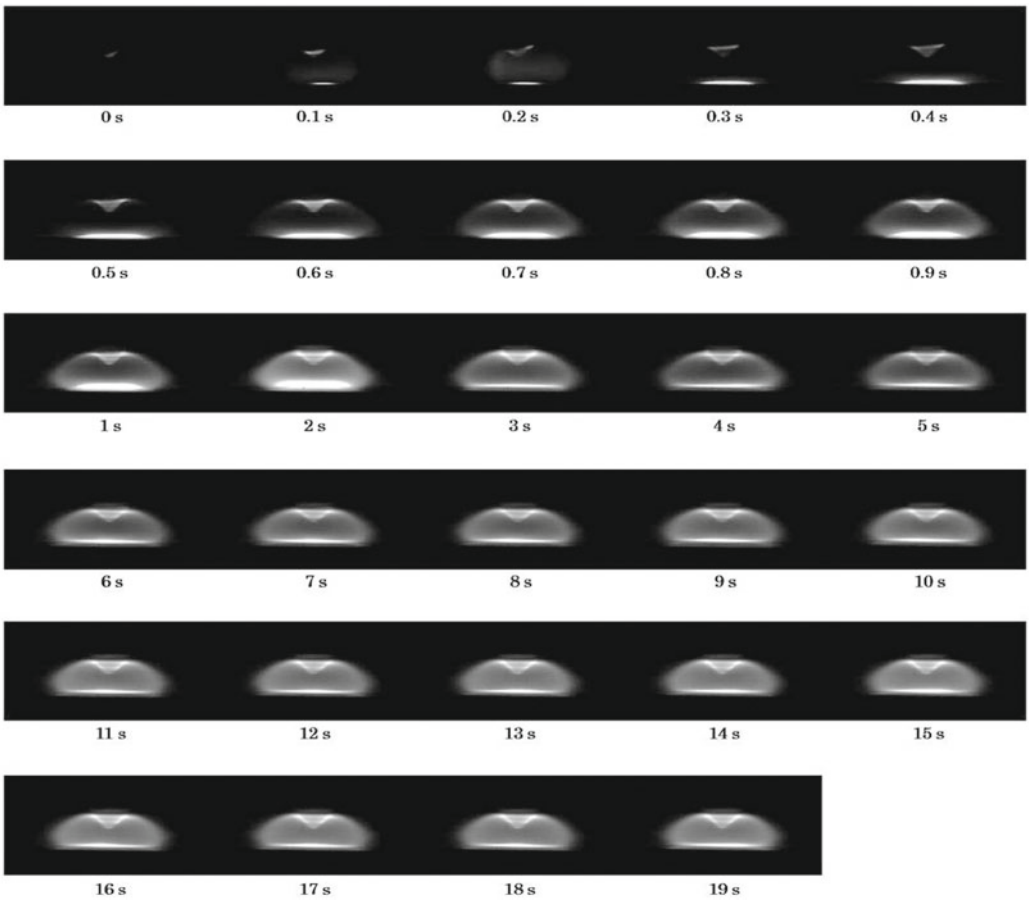

Figure 4 – Photographs of MnI spectrum in arc during helium TIG welding of stainless steel

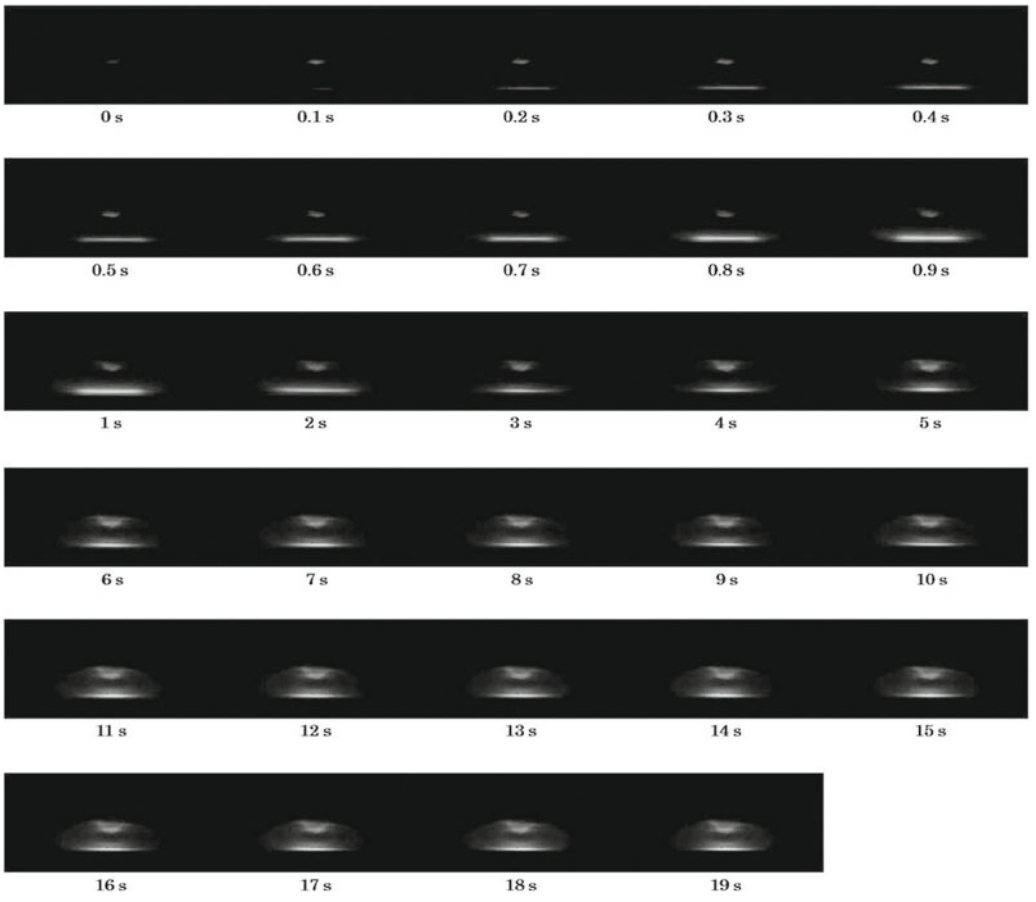

Figure 5 – Photographs of FeI spectrum in arc during helium TIG welding of stainless steel

4 Observations at electrodes

Figure 7 shows analytic results of elemental mapping of the tungsten electrode by FE-SEM after stationary TIG welding of stainless steel for 20 s. A lot of chromium exists on the surface of the tungsten electrode at about 1.7 mm and more away from the tungsten electrode tip. Manganese and iron cannot be detected and are negligible.

A two-colour pyrometry with a high-speed digital video camera has been conducted to obtain the surface temperature of the tungsten electrode [20]. Figure 8 shows

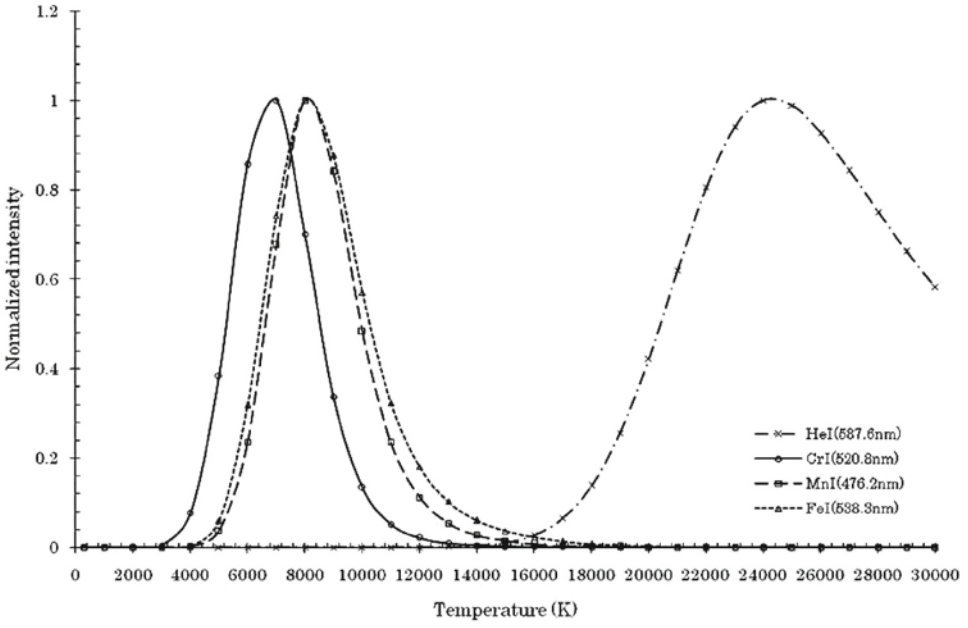

Figure 6 – Dependence of normalized radiant intensities on temperature for HeI, CrI, MnI and FeI spectra

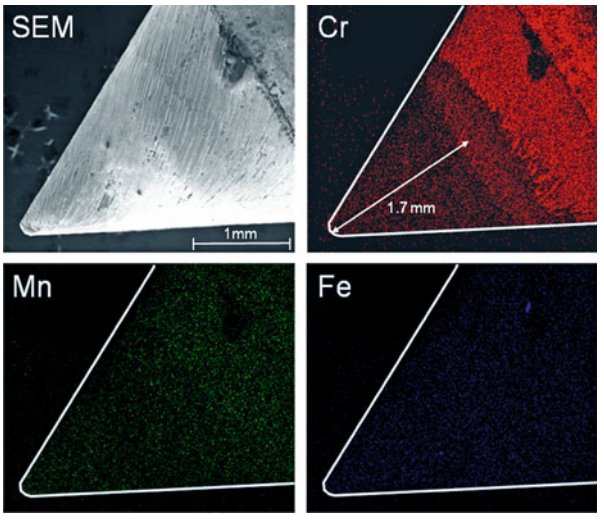

Figure 7 – Results of elemental analysis of the tungsten electrode after TIG welding of stainless steel for 20 s

the axial temperature distribution of the tungsten electrode. The boiling points of chromium, manganese and iron are 2 933 K, 2 305 K and 3 160 K, respectively [18]. The tungsten electrode surface temperature is about 3 500 K at the electrode tip and is reduced by 3 000 K at 1.7 mm from the tip as shown in Figure 8. A comparison of the boiling point of chromium and the result of Figure 8 shows the presence of chromium where the tungsten electrode surface temperature is less than the boiling point. However, manganese can hardly be present because of its low boiling point. Although the tungsten electrode surface temperature becomes lower than the boiling point of iron (about 3 200 K) at about 1.6 mm and more from the tip, iron has not the same tendency with chromium. From these results, it can be concluded that there is little iron vapour inside the arc plasma.

On the other hand, smut on the stainless steel after the stationary TIG welding is analysed quantitatively. Figure 9 shows the results of the quantitative smut analysis by EDAX (Energy Dispersive Analysis of X-ray). The smut consists of a great quantity of manganese and iron which

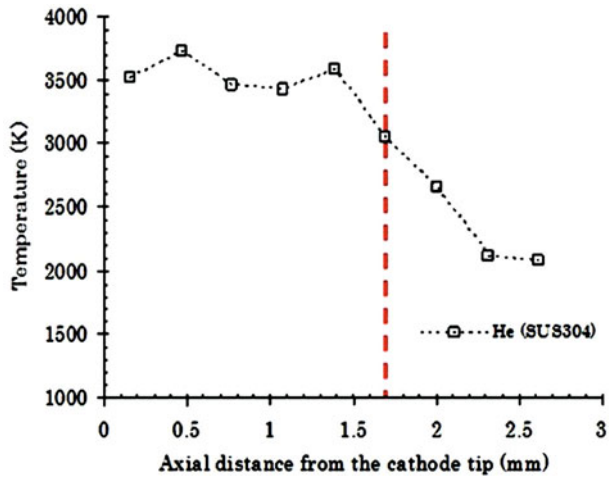

Figure 8 – Axial temperature distribution of tungsten electrode during TIG welding of stainless steel

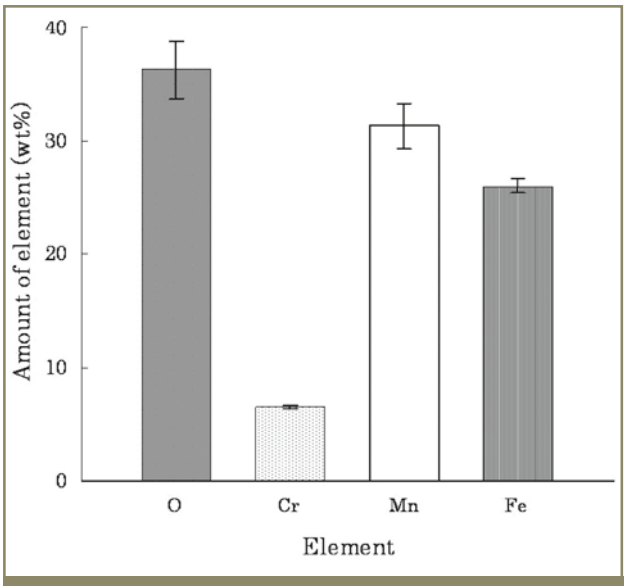

Figure 9 – Result of quantitative smut analysis by EDAX after TIG welding of stainless steel for 20 s

are hardly detected on the surface of the tungsten electrode, and also consists of a little chromium.

5 Discussion

In the TIG arc, the current density at the tungsten cathode tip is much higher than on the base metal, and then a strong plasma fluid flows from cathode to anode, i.e., the cathode jet occurs [21]. Most of the metal vapour from the weld pool surface is swept away towards surroundings of the arc plasma by the cathode jet.

Results of calculations by Ushio [22] show that arc plasma has not only the cathode jet, but also a convective circulation flow. It is suggested that part of the metal vapour can be carried by this circulation flow towards the tungsten electrode. And then, the metal vapour can be transported into the arc column, as shown in Figure 10.

Metal vapour diffusion in plasma is one of the driving forces leading metal vapour into the arc plasma. Metal

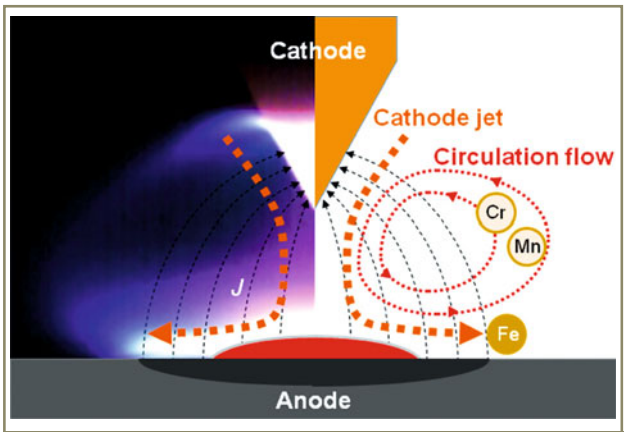

Figure 10 – Illustration of convective circulation flow in TIG arc

vapour diffusion in plasma [23] is given by the following equation,

$$\overline{J_A} = \frac{n^2}{\rho}\overline{m_A}\,\overline{m_B}\left(\overline{D^x_{AB}}\nabla\overline{x_B} + \overline{D^E_{AB}}E\right) - \overline{D^T_{AB}}\nabla \ln T \qquad (1)$$

where

n and ρ are respectively the number density and mass density of gas,

E is the electrical field,

T is the temperature,

$\overline{m_A}$ and $\overline{m_B}$ are respectively the average mass of the heavy particles of gas A and gas B,

$\nabla\overline{x_B}$ is the sum of mole fractions of all species of gas B,

$\overline{D^x_{AB}}$, $\overline{D^E_{AB}}$ and $\overline{D^T_{AB}}$ are respectively the combined diffusion coefficients for ordinary, electrical field and thermal diffusion. The first term shows ordinary diffusion by concentration gradient, the second term shows diffusion by potential gradient, and the third term shows diffusion by temperature gradient. Diffusion by temperature gradient is small and then negligible in low temperature regions like a weld pool surface [24]. Diffusion coefficient of metal element increases with increasing metal element concentration, and metal vapour becomes easy to diffuse. Large amount s of manganese can evaporate because of its lower boiling point. Therefore, diffusion by concentration gradient has the most effect for manganese vapour in other metal elements. Ionization energies of chromium, manganese and iron are 6.77 eV, 7.43 eV, and 7.90 eV, respectively. The chromium ionization energy is about 0.7 ~ 1.1 eV less than that of the other metal elements. In particularly low-temperature plasma close to the weld pool surface, chromium would be preferentially ionized in comparison with manganese and iron. Therefore, it is considered that diffusion by potential gradient has the most effect for chromium vapour.

In the TIG arc, there is not only the cathode jet but also a convective circulation flow, as shown in Figure 10 [22]. This convective circulation flow is an upper stream in comparison with the cathode jet on the weld pool surface. Most of the metal vapour produced from the weld pool surface is swept away towards surroundings of the arc plasma by the cathode jet. However, some of the metal vapour is affected by a driving force like diffusion. If the driving force by diffusion is so large, some metal elements can get across the cathode jet and reach the circulation flow situated on the upper stream of the cathode jet. Then, these metal elements are carried on the circulation flow towards the tungsten electrode. It is thought that chromium and manganese vapours can mix in the arc plasma through the circulation flow due to the diffusion on the weld pool surface. Dominant diffusion driving forces are the concentration gradient for manganese and the potential gradient for chromium. However, iron vapour cannot diffuse into the circulation flow across the cathode jet and then is swept away towards surroundings of the arc plasma by the cathode jet, because of the low iron vapour concentration in the arc plasma close to the weld pool surface due to its higher boiling point; also there are hardly iron ions in the arc plasma close to the weld pool surface due to the higher ionization energy.

6 Conclusions

The conclusions of this work are summarized as follows.

1. Intensity of HeI spectrum weakens with passing time because plasma temperature decreases due to metal vapour in the arc plasma.
2. Large amounts of manganese and chromium vapour are present in the arc plasma whereas small amounts of iron vapour are present.
3. Chromium diffuses easily by potential gradient due to its lower ionization energy and chromium vapour from the weld pool surface mixes in the arc plasma through a convective circulation flow in the arc.
4. Large quantities of manganese can evaporate due to its lower boiling point. Therefore, manganese diffuses easily by concentration gradient and manganese vapour from the weld pool surface can mix in the arc plasma through a convective circulation flow in the arc.
5. Iron vapour from the weld pool surface is swept away towards surroundings of the arc plasma by the cathode jet, because the driving force of iron to diffuse is too weak to mix in the arc plasma due to its higher boiling point and also higher ionization energy.

Acknowledgements

This work was supported by KAKENHI 22246095, Grant-in-Aid for Scientific Research (A).

References

[1] Tanaka M. and Lowke J.J.: Predictions of weld pool profiles using plasma physics, Journal of Physics D: Applied Physics, 2007, vol. 40, no. 1, pp. R1-R24.

[2] Fauchais P.: Understanding plasma spraying, Journal of Physics D: Applied Physics, 2004, vol. 37, no. 9, pp. R86-R108.

[3] Nemchinsky V.A. and Severance W.S.: What we know and what we do not know about plasma cutting, Journal of Physics D: Applied Physics, 2006, vol. 39, no. 22, pp. R423-R438.

[4] Hirsh M.N. and Oskam H.J.: Gaseous Electronics, 1978, Academic Press, New York.

[5] Lancaster J.F.: Physics of Welding, 1984, Pergamon Press, Oxford.

[6] Boulos M.I., Fauchais P. and Pfender E.: Thermal Plasmas, 1994, Plenum Press, New York.

[7] Etemadi K. and Pfender E.: Impact of anode evaporation on the anode region of high-intensity argon arc, Plasma Chemistry and Plasma Processing, 1985, vol. 5, no. 2, pp. 175-182.

[8] Dunn G.J., Allemand C.D. and Eagar T.W.: Metal vapors in gas tungsten arcs: Part I. Spectroscopy and monochromatic photography, Metallurgical and Materials Transactions A, 1986, vol. 17, no. 10, pp. 1851-1863.

[9] Dunn G.J. and Eagar T.W.: Metal vapors in gas tungsten arcs: Part II. Theoretical calculations of transport properties, Metallurgical Transactions A, 1986, vol. 17, no. 10, pp.1865-1871.

[10] Farmer A.J.D., Haddad G.N. and Cram L.E.: Temperature determinations in a free-burning arc: III. Measurements with molten anodes, Journal of Physics D: Applied Physics, 1986, vol. 19, no. 9, pp. 1723-1730.

[11] Yamamoto K., Tanaka M., Tashiro S., Nakata K., Yamazaki K., Yamamoto E., Suzuki K. and Murphy A.B.: Metal vapour behaviour in thermal plasma of gas tungsten arcs during welding, Science and Technology of Welding & Joining, 2008, vol. 13, no. 6, pp. 566-572.

[12] Murphy A.B., Tanaka, Yamamoto K., Tashiro S., Sato T. and Lowke J.J.: Modelling of thermal plasmas for arc welding: the role of the shielding gas properties and of metal vapour, Journal of Physics D: Applied Physics, 2009, vol. 42, no. 19, p. 194006.

[13] Schnick M., Fussel U., Hertel M., Spille-Kohoff A. and Murphy A.B: Metal vapour causes a central minimum in arc temperature in gas-metal arc welding through increased radiative emission, Journal of Physics D: Applied Physics, 2010, vol. 43, no. 2, p. 022001.

[14] Tanaka M., Yamamoto K., Tashiro S., Nakata K., Yamamoto E., Yamazaki K., Suzuki K., Murphy A.B. and Lowke J.J.: Time-dependent calculations of molten pool formation and thermal plasma with metal vapour in gas tungsten arc welding, Journal of Physics D: Applied Physics, 2010, vol. 43, no. 43, p. 434009.

[15] Zielinska S., Musiol K., Dzierzega K., Pellerin S., Valensi F., de Izarra Ch. and Briand F.: Investigation of GTAW plasma by optical emission spectroscopy, Plasma Sources Science and Technology, 2007, vol. 16, no. 4, pp. 832-838.

[16] Wiese W.L., Smith M.W. and Miles B.M.: Atomic transition probabilities, 1966, NSRDS, National Standard Reference Data Series, Washington.

[17] Terasaki H., Tanaka. M. and Ushio M.: Effects of metal vapour on electron temperature in helium gas tungsten arcs, Metallurgical and Materials Transactions A, 2002, vol. 33, no. 4, pp. 1183-1188.

[18] The Japan Institute of Metals: Data Book of Metals, 1993, Maruzen, Tokyo.

[19] National Institute of Standards and Technology (NIST): Atomic Spectra Database, 2008, http://www.nist.gov/pml/data/asd.cfm

[20] Tashiro S. and Tanaka M.: Effect of admixture of metal vapour on cathode surface temperature of plasma torch, Surface and Coatings Technology, 2008, vol. 202, no. 22-23, pp. 5255-5258.

[21] Tanaka M. and Ushio M.: Plasma state in free-burning argon arc and its effect on anode heat transfer, Journal of Physics D: Applied Physics, 1999, vol. 32, no. 10, pp. 1153-1162.

[22] Ushio M. and Matsuda F.: A Mathematical modeling of flow and temperature fields in gas-tungsten-arc, Quarterly Journal of the Japan Welding Society, 1988, vol. 6, no. 1, pp. 91-98.

[23] Murphy A.B.: Cataphoresis in electric arcs, Journal of Physics D: Applied Physics, 1998, vol. 31, no. 23, pp. 3383-3390.

[24] Murphy A.B.: A comparison of treatments of diffusion in thermal plasmas, Journal of Physics D: Applied Physics, 1996, vol. 29, no. 7, pp. 1922-1932.

About the authors

Prof. Dr. Manabu TANAKA (tanaka@jwri.osaka-u.ac.jp) and Mr. Yoshihiro TSUJIMURA (tujimura@jwri.osaka-u.ac.jp) are both with Joining and Welding Research Institute, Osaka University, Osaka (Japan). Mr. Kei YAMAZAKI (yamazaki.kei@kobelco.com) is with Kobe Steel, Ltd., Kanagawa (Japan).